Journal of Hazardous Materials 168 (2009) 1070–1081

Contents lists available at ScienceDirect

Journal of Hazardous Materials

journal homepage: www.elsevier.com/locate/jhazmat

Activated carbon from agricultural by-products for the removal of Rhodamine-B from aqueous solution

Hamdi M.H. Gad*, Ashraf A. El-Sayed

Hot Laboratories and Waste Management Centre, Egyptian Atomic Energy Authority, P.O. 13759, Cairo, Egypt

ARTICLE INFO

Article history:
Received 27 September 2008
Received in revised form 26 February 2009
Accepted 27 February 2009
Available online 13 March 2009

Keywords:
Activated carbon
Bagasse pith
Rhodamine B
Isotherm models
Desorption

ABSTRACT

Bagasse pith (BP) has been utilized for activated carbon preparation using H_3PO_4 (BPH) or KOH (BPK) as a chemical activating agent followed by carbonization at 500 °C. The physicochemical properties of activated carbon were carried out. The effectiveness of carbon prepared in adsorption of Rhodamine B (RhB) has been studied as a function of adsorbent type, pH, particle size, agitation time, temperature, initial dye concentration, and desorption. The results obtained showed that the adsorb ability of (RhB) to the BPH is higher than that of the BPK carbon by approximately 10 folds (198.6 and 21.5 mg g^{-1}, respectively). Kinetic studies show that the adsorption of RhB proceeds according to the pseudo-second-order. The intra-particle diffusion was identified to be the rate-limiting step in addition to the film diffusion. The adsorption was analyzed using 5 isotherm models (Langmuir, Freundlich, Temkin, Harkins–Jura, and Halsey isotherm equations). The highest values of r^2 were obtained with Langmuir (0.997). The adsorption capacity, q_m, was 263.85 (mg g^{-1}) at initial pH 5.7 for the particle size 0.25 nm and equilibrium time of 240 min at a temperature of 20 °C and initial dye concentration range of 100–600 (mg l^{-1}). Temperature effect proves that the adsorption is endothermic with $\Delta H = 4.151$ (kJ mol^{-1}), $\Delta S = 65.786$ (J mol^{-1} K^{-1}) and a decrease in Gibbs energy ($\Delta G = -7.939$ to -26.729 kJ mol^{-1}). Desorption studies were carried out using water medium, HCl and NaOH with desorption of 2.7, 5.4 and 7.8%, respectively of adsorbed RhB confirming the chemical adsorption mechanism of the dye. This adsorbent was found to be both effective and economically viable.

1. Introduction

Color is the first contaminant to be recognized in water and has to be removed from wastewater before discharging it into water bodies. Residual dyes are the major contributors to color in wastewaters generated from textile and dye manufacturing industries, etc. [1]. Color impedes light penetration, retards photosynthetic activity, inhibits the growth of biota and also has a tendency to chelate metal ions which result in micro-toxicity to fish and other organisms [2]. It should be noted that the contamination of drinking water by dyes at even a concentration of 1.0 mg l^{-1} could impart significant color, making it unfit for human consumption [1]. Most of the used dyes are stable to photo-degradation, bio-degradation and oxidizing agents [2]. Currently, several physical or chemical processes are used to treat dye-laden wastewaters. However, these processes are costly and cannot be used effectively to treat the wide range of dye-laden wastewater. The advantages and disadvantages of some methods of dye removal from wastewaters are given in Table 1 [3]. The adsorption process is one of the efficient methods to remove dyes from effluent and has an advantage over the other methods due to the excellent adsorption efficiency of activated carbon (powdered or granular) for organic compounds even from dilute solutions, but commercially available activated carbons are very expensive.

Various carbonaceous materials, such as coal, lignite, coconut shells, wood and peat are used in the production of commercial activated carbons [4]. However, the abundance and availability of agricultural by-products make them good sources of raw materials for activated carbons. Agricultural by-products [5] are renewable sources of raw materials for activated carbon production because the development of methods to reuse waste materials is greatly desired. Residues from agriculture and agro-industries are the non-product outputs from the growing and processing of raw agricultural products such as rice, corn, beans and peanuts [6]. Disposal of agricultural by-products is currently a major economic and ecological issue, and the conversion of by-products to adsorbents, such as activated carbon, represents a possible outlet. A number of agricultural waste materials are being studied for the removal of different dyes from aqueous solutions at different operating conditions (Table 2; [1]). Activated carbon prepared from bagasse pith is a promising adsorbent for the removal of dyes from wastewater [28,44,45]. In Egypt, this agricultural by-product is produced

* Corresponding author.
E-mail address: hmhgad1@yahoo.com (H.M.H. Gad).

0304-3894/$ – see front matter.
doi:10.1016/j.jhazmat.2009.02.155

Table 1
Advantages and disadvantages of the methods used for dye removal from industrial effluents [3].

Physical/chemical methods	Advantages	Disadvantages
Fentons reagent	Effective decolorization	Sludge generation
Ozonation	No change in effluent volume	Short half life (20 min)
Photochemical	No sludge generation	Formation of by-products
NaOCl	Initiate azo-bond cleavage	Release of aromatic amines
Electrochemical	Non-hazardous end products	High cost of electricity
Activated carbon	Highly effective for various dyes	Very expensive
Peat	Good adsorbent	Surface area is low
Silica gel	Effective for basic dyes	Side reactions in effluent
Membrane filtration	Removes all dyes	Concentrated sludge production
Ion exchange	No adsorbent loss	Not effective for all dyes

in huge amount continuously. This by-product is a carbonaceous, and fibrous solid waste, which creates a disposal problem and is generally used for its fuel value. Therefore, it was of interest to prepare a higher value product, such as activated carbon, from it.

The high adsorptive capacities of activated carbons are related to properties such as surface area, porosity, and surface functional groups. These unique characteristics are dependant on the type of raw material employed and method of activation. Basically, there are two different processes for the preparation of activated carbon: physical and chemical activation [7]. Physical activation involves carbonization of the carbonaceous precursor followed by activation of the resulting char in the presence of activating agents such as carbon dioxide or steam. Chemical activation, on the other hand, involves the carbonization of the precursor in the presence of chemical agents. In physical activation, the elimination of a large amount of internal carbon mass is necessary to obtain a well-developed porous structure, whereas in chemical activation process, chemical agents used are dehydrating agents that influence pyrolytic decomposition and inhibit the formation of tar, thus enhancing yield of carbon. Chemical activation has more advantages [8], over physical activation with respect to higher yield, more surface area and better development of porous structure in carbon. It also helps to develop oxygenated surface complexes on the surface of activated carbon. Consequently, the aim of this work was to study the feasibility of developing an efficient adsorbent from agricultural by-product by H_3PO_4 (or KOH) activation and to investigate its adsorption capacity by removal of dye from aqueous solutions.

RhB was selected for the adsorption experiment due to its presence in the wastewaters of several industries (such as textile, leather, jute and food industries). Detection of gamma rays is now a days using the photosensitive dye, which changes its color with incident radiation. To evaluate the suitability of the prepared activated carbon for its use in water and wastewater treatment systems, its characterization has been done for physical, chemical and adsorption properties because these preliminary studies provide good information about the applicability of the product in a treatment system.

2. Experimental

2.1. Adsorbent raw material

In the manufacture of sugar, the sugar cane stalks are chopped to small pieces by rotary knives, and juice is extracted by crushing them through one or more roller mills. During this process more than 95% of sucrose content of the cane is removed. The waste residual material from this operation is termed bagasse pith. The moisture content of bagasse pith was $14.5 \pm 0.5\%$ [9], and it was not subjected to any form of pretreatment prior to use. The Egyptian bagasse pith was subjected to chemical analysis [10] and the results obtained are given in Table 3.

2.2. Preparation of activated carbon

Bagasse pith (BP) was chosen as precursor for the production of activated carbons by one-step chemical activation using H_3PO_4 (or KOH). In each experiment, 60 g of crushed bagasse pith was soaked in 100 ml of 70% H_3PO_4 (or KOH) solution to cover it completely, slightly agitated to ensure penetration of the acid (or base) throughout, then the mixture was heated to 80 °C for 1 h and left overnight at room temperature to help appropriate wetting and impregnation of the precursor. The impregnated mass was dried in an air oven at 80 °C overnight, then, admitted into the reactor (ignition tube), which was then placed in a tubular electric furnace open from both ends. The temperature was raised at the rate of (50 °C/10 min.) to the required end temperature. The carbonization process was carried out at 500 °C for 80 min in limited air. The product – (BPH) refers to H_3PO_4 treatment, whereas (BPK) refers to KOH treatment – was thoroughly washed with warm distilled water (70 °C) until pH of the solution came close to the initial pH of the rinsing water. Finally, the activated carbon was dried at 110 °C for 24 h and sieved to different particle sizes and kept for use.

2.3. Characterization of prepared BPH activated carbon

The resulting carbon was then characterized with respect to its pore structure and surface area using nitrogen

Table 2
Some agricultural wastes studies for dye(s) removal from aqueous solutions [1].

No.	Agricultural waste	Dye(s)
1	Maize cob	Astrazon blue, Erionyl red
2	Coconut shell, groundnut shell	Methylene blue
3	Silk, cotton hull, coconut tree sawdust, maize cob	Rhodomine-B, congo red, methylene blue, methyl violet, malachite green
4	Rice husk	Malachite green, basic, acid direct and disperse dyes, acid yellow 36, saframnine, methylene blue
5	Orange peel	Acid violet 17
6	Coir pith	Acid violet, acid brilliant blue, methylene blue, Rhodomine-B, congo red
7	Banana and orange peels	Methylene orange, methylene blue, methyl violet, acid black, Congo red, Rhodamine-B, procion orange
8	Banana pith	Congo Red, Rhodamine-B, acid violet, acid brilliant blue, acid brilliant blue
9	Groundnut shell powder	Basic, direct and disperse dyes
10	Wheat straw, corncob, bark husk.	Cibacron yellow C-2R, cibacron red C-2G, cibacron blue C-R, remazol black B, remazol red RB.

Table 3
Physicochemical characterization of BPH activated carbon and chemical analysis of bagasse pith.

No.	Parameters	Values	No.	Parameters	Values
1	Carbon yield (%)	95	15	Phenol number (mg)	150
2	Ash content (%)	6.5	16	Iodine number ($mg\,g^{-1}$)	740
3	Methylene blue number ($mg\,g^{-1}$)	280	17	Particle size (mm)	1.0–0.25
4	Packed density ($g\,ml^{-1}$)	0.284	18	Matter soluble in water (%)	1.7
5	Apparent density ($g\,ml^{-1}$)	0.17	19	Matter soluble in acid (%)	2.42
6	BET surface area ($m^2\,g^{-1}$)	522.7	20	Matter soluble in base (%)	2.31
7	Langmuir surface area ($m^2\,g^{-1}$)	797	21	Moisture content (%)	6
8	Average pore radius (Å)	15.04	22	C %	75.76
9	Half pore width (Å)	7.374	23	H %	3.56
10	Micropore surface area ($m^2\,g^{-1}$)	589.6	24	N %	2.1
11	Total pore volume ($cm^3\,g^{-1}$)	0.388	25	S %	0.6
12	Micropore volume ($cm^3\,g^{-1}$)	0.091	26	O % (by difference)	16.98
13	Mesopores volume ($cm^3\,g^{-1}$)	0.297	27	pH	3.5
14	Point of zero charge (pH_{PZC})	3.9	28		
Chemical analysis of bagasse pith raw material %					
1	α-Cellulose	53.7	4	Alcohol/benzene solubility	7.5
2	Pentosan	27.9	5	Ash	6.6
3	Lignin	20.2			

adsorption/desorption at −196 °C which was conducted using a gas sorption analyzer (Quantachrome, NOVA 1000e series, USA), pH, elemental analysis, ash content, density, solubility in water, acid and base.

2.4. Adsorption procedure

The sorption study was performed by batch sorption experiments using RhB as an adsorbate and bagasse pith activated carbon as an adsorbent. The properties of RhB are presented in Table 4. The dye was made up in stock solutions of concentration $1000\,mg\,l^{-1}$ and was subsequently diluted to required concentrations ($100–600\,mg\,g^{-1}$). Calibration curve for dye was prepared by recording the absorbance values for a range of known concentrations at the wavelength for maximum absorbance. This value, λ_{max}, was found to be 554 nm for RhB. The pH of the solution was adjusted using HCl and NaOH and all pH measurements were carried out using a digital pH meter. Temperature controlled shaking thermostat was used to control the desired temperature. The effect of experimental parameters such as pH value, temperature, different particle sizes of carbon and concentration were studied. Blanks were run simultaneously without any sorbent.

Adsorption experiments were conducted by adding 100 mg of activated carbons into a series of 250 ml Erlenmeyer each filled with 100 ml of experimental solution with each initial concentration, particle size of carbon, pH and temperature. All of the Erlenmeyer were then covered with aluminum foil and placed to a thermostatic shaker bath and shaken to eqilibrium. After equilibrium time had been reached, activated carbon was separated from the solution by centrifugation at 3000 rpm for 5 min. The absorbance of clarified supernatant solution was analyzed using a UV–vis spectrophotometer (Shimadzu 160-A Model). The amount of adsorbed RhB [uptake ($mg\,g^{-1}$) at time t, q_t], was calculated from the mass balance equation:

$$q_t = C_e - C_t \times \frac{V}{M} \quad (1)$$

when t is equal to the equilibrium contact time, $C_t = C_e$, $q_t = q_e$, and the amount of adsorbed at equilibrium, q_e, is calculated using Eq. (1).

Table 4
Properties of Rhodamine-B.

Parameters	Values	Parameters	Values
Suggested name	Rhodamine-B	Solubility in water	0.78%
C.I. number	45170	Solubility in ethanol	1.47%
C. I. name	Basic violet 10	Absorption maximum	56.5
Class	Rhodamine	Empirical formula	$C_{28}H_{31}N_2O_3Cl$
Ionization	Basic	Formula weight	479.029
Color	Red		

2.5. Desorption studies

After adsorption experiments the RhB laden carbon was separated out by filtration using Whattman filter paper no. 42 and the filtrate was discarded. The RhB loaded carbon was given a gentle wash with double-distilled water to remove the unadsorbed RhB if present. Desorption studies were carried out using several such carbon samples. They were agitated with distilled water, NaOH or HCl solution of 0.1N concentration. The desorbed RhB in the solution was separated by centrifugation and analyzed as before.

3. Results and discussion

Neither changes appeared in the absorption spectrum nor additional peaks formed for the dye solution after shaking it with the adsorbent. This indicated that there was no breakdown product(s) of the dye and also supported the fact that the dye removal from the solution in this study was through the mechanism of adsorption [11].

In activated carbon–liquid phase interactions, it has been known that the adsorption capacity depends on a number of factors namely: (a) the physical nature of the adsorbent-pore structure, ash content and functional groups; (b) the nature of the adsorbate, its p*K*a, functional groups present, polarity, molecular weight and size; (c) the solution conditions such as pH, ionic strength and the adsorbate concentration. In the following sections we will investigate some of these factors.

3.1. Characterization of BPH activated carbon

Pore characteristic of the activated carbon was determined by N_2 adsorption. The nitrogen adsorption/desorption isotherms of BPH activated carbon is illustrated in Fig. 1. The activated carbon possessed combination of type I and type II of IUPAC isotherm, indicating simultaneous presence of micropores and mesopores. This isotherm also exhibited a type H4 hysteresis loop, characteristic of slit-shaped pores. The pore characteristics of BPH activated

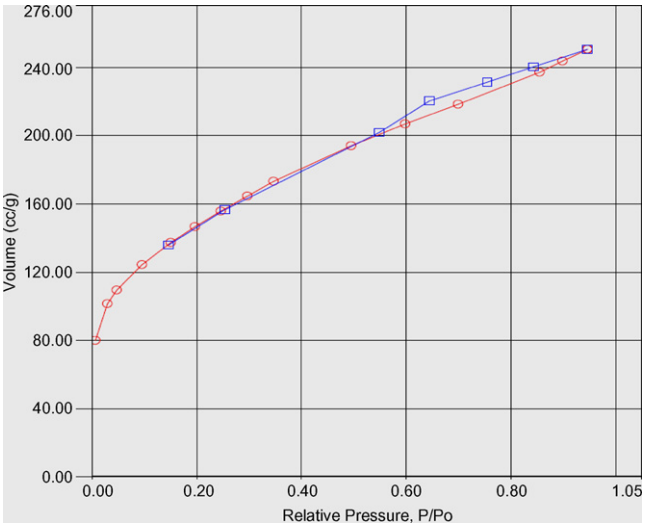

Fig. 1. Nitrogen adsorption/desorption isotherm of BPH activated carbon.

carbon are given in Table 3. The presence of micropores and mesopores in the activated carbon prepared from bagasse pith were also indicated by the pore size distribution as depicted in Fig. 2. A proximate analysis of the BPH was carried out, using the recommended standard methods of analysis. The physicochemical characterization of BPH activated carbon and its precursor (bagasse pith) is summarized in Table 3.

3.2. The effect of adsorbent surface change

The BP treated with H_3PO_4 has larger capacity compared to the BP treated with KOH, as shown in Fig. 3. The treatments with acid produce three types of surface oxides: acidic, basic, and neutral [12]. Fixation of the acidic groups on the surface of the activated carbon makes it more hydrophilic and decreases its pH of the point of zero charge [13]. Puri and Mahajan [14] have reported that the replacement of alkaline ions with H^+ on charcoal causes the hydrophobicity of the surface of the carbon to increase. So, in our study, the adsorbability of RhB to the BPH carbon is higher than that of the BPK carbon by approximately 10 folds (198.6 and 21.5 mg g^{-1}, respectively). Two agents (H_3PO_4 and KOH) can produce different surface properties. Higher adsorption capacity of BPH indicates two possibilities; one is that the hydrophobicity and hyrophilicty of the carbon surface have no effect on the adsorption;

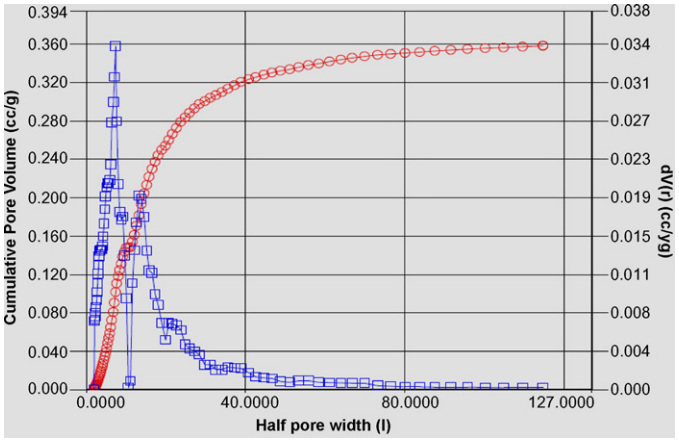

Fig. 2. Pore size distribution of BPH activated carbon.

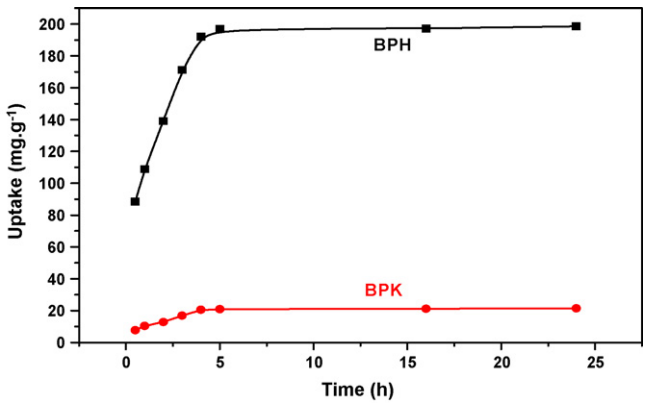

Fig. 3. Effect of activating agent on the adsorption of RhB.

the other is that they are all fit for the adsorption process, as the RhB ions have different functional groups. From the obtained results, the BPH carbon was used in the further investigation of the factors affecting of on the adsorption of RhB.

3.3. Effect of pH

The effect of pH on the adsorption of RhB ions onto BPH carbon was determined. The result is shown in Fig. 4. The experimental data showed that the uptake of RhB at pH 2.45 was 190.8 (mg g^{-1}) and it has been observed that the uptake decreases with increase in pH. As shown, at pH 3.44 the uptake was 187.9(mg g^{-1}) where, at pH 10 the RhB uptake was 168.7 (mg g^{-1}). The influence of pH on the pronounced sorption of RhB on the surface of the carbon at low pH ranges leads to the assumption that chemisorptions dominates in this range and chemisorptions along with physisorption occurs at higher pH ranges [15]. In addition, it appears that a change in pH of the solution results in the formation of different ionic species, and different carbon surface charge. At pH values lower than 4, the RhB ions are of cationic and monomeric molecular form [16], thus theyRhB can enter into the pore structure. At a pH value higher than 4, the zwitterionic form of RhB in water (Fig. 5) may increase the aggregation of RhB to form a larger molecular form (dimer) and become unable to enter into the pore. Ghanadzadeh et al. [17] have studied the aggregation of RhB in the microporous solid hosts. Lopez Arbeloa and Ruiz Ojeda [18] determined the equilibrium constant for the dimer ↔ monomer transition of RhB in aqueous solution. The greater aggregation of the zwitterionic form is due to the attractive electrostatic interactions between the carboxyl and xanthene groups of the monomers [19].

3.4. Effect of contact time and initial dye concentration

Very rapid adsorption was found during the adsorption time of 4 h. However, the amount of RhB adsorbed increases with time and reaches a constant value after 5 h. After the equilibrium time, the amount of RhB adsorbed did not alter with time. Thus, the mixing time for the rest of adsorption studies was set to be 5 h to ensure the equilibrium in adsorption and kinetic studies. The amount of RhB dye adsorbed per unit mass of BPH activated carbon increased with increase in dye concentration in test solution. It increased from 100 to 264 mg g^{-1} as the RhB concentration in the test solution was increased from 100 to 600 mg l^{-1}. Maximum dye was sequestered from the solution within 4 h after the start of every experiment. After that, the concentration of RhB in liquid phase remained almost constant. In the process of dye adsorption initially dye molecules have to first encounter the boundary layer effect and

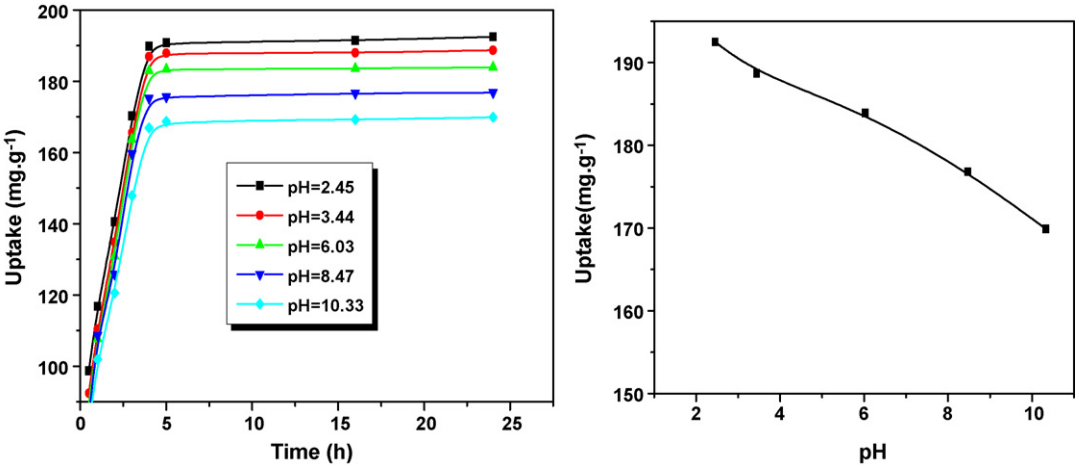

Fig. 4. Effect of initial pH solution on the adsorption of RhB onto BPH activated carbon.

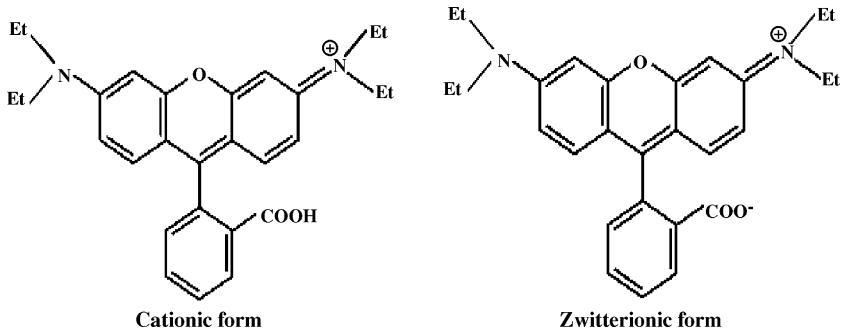

Fig. 5. Molecular form of RhB (cationic and zwitterionic form).

then they have to diffuse from boundary layer film onto adsorbent surface and then finally, they have to diffuse into the porous structure of the adsorbent. For higher initial concentration studied, it was found that there was no significant change on the equilibrium time at the observed initial RhB concentration range. The uptake ($mg\,g^{-1}$) of dye removal versus time curves is single, smooth and continuous leading to saturation(Fig. 6), suggesting the possibility of monolayer coverage of RhB on the outer surface of the BPH activated carbon[20]. These observations are consistent with the observations of other results [21,22] for the biosorption of basic dyes by water hyacinth, duckweed and sawdust.

3.5. Kinetic of adsorption of RhB onto BPH activated carbon

In order to investigate the mechanism of sorption and potential rate-controlling steps such as mass transport and chemical reaction processes, kinetic models have been used to test experimental data. These kinetic models included the pseudo-first order, the pseudo-second-order and the Elovich equations.

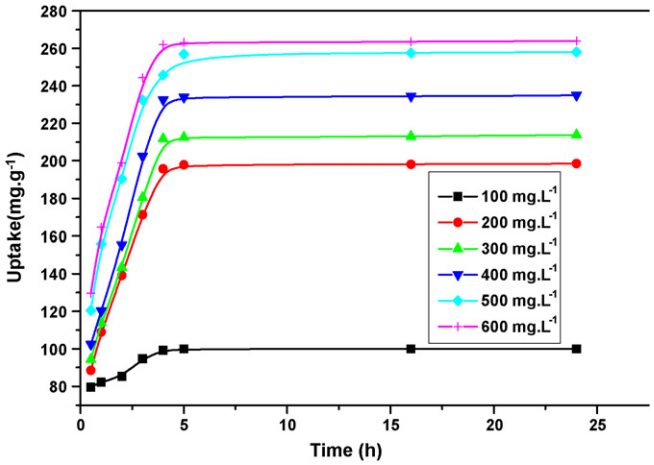

Fig. 6. Effect of contact time and initial dye concentration on the adsorption of RhB onto BPH activated carbon.

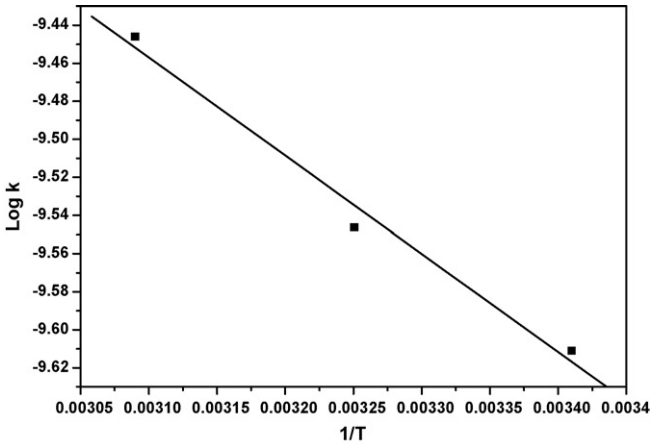

Fig. 7. Plot of log k_c against reciprocal temperature for RhB sorption onto BPH activated carbon.

Table 5
Kinetic of adsorption of RhB onto BPH activated carbon: first-order constants for the effect of pH, particle sizes, concentration and temperature.

Parameter	Values	First-order equation $\log(q_e-q_t)=\log(q_e)-k_1/2.303.t$				
		$q_{e,}$ exp. mg g^{-1}	q_e Calcu. mg g^{-1}	K_1 (min^{-1})	r^2	Slope X10^{-3}
pH	2.45	192.5	219.8	16.1×10^{-3}	0.965	6.96
	3.44	188.7	283.9	18.7×10^{-3}	0.957	8.16
	6.03	183.9	319.3	20.9×10^{-3}	0.951	9.08
	8.47	176.8	277.1	17.6×10^{-3}	0.960	7.65
	10.33	169.9	214.9	16.4×10^{-3}	0.965	7.13
Particle size (mm)	<0.25	200.0	355.2	20.8×10^{-3}	0.961	9.06
	<0.50	192.5	261.5	18.8×10^{-3}	0.971	8.20
	<1.00	188.7	280.3	18.2×10^{-3}	0.978	7.92
Concentration (mgl^{-1})	100	100.0	46.60	14.6×10^{-3}	0.928	6.35
	200	198.6	337.1	18.9×10^{-3}	0.958	7.10
	300	213.8	345.2	18.2×10^{-3}	0.947	7.90
	400	235.0	419.9	19.2×10^{-3}	0.955	8.24
	500	258.0	330.4	18.4×10^{-3}	0.952	8.33
	600	264.0	373.8	19.7×10^{-3}	0.972	8.55
Temperature (°C)	20	192.6	364.1	21.8×10^{-3}	0.945	9.48
	35	195.9	350.3	20.4×10^{-3}	0.959	8.87
	50	199.6	280.7	18.1×10^{-3}	0.965	7.87
	70	218.8	196.12	11.9×10^{-3}	0.974	5.17

3.5.1. Pseudo-first order reaction

The pseudo-first order equation of Lagergren [23] is generally expressed as follows:

$$\log(q_e - q_t) = \log(q_e) - \frac{k_1}{2.303.t} \quad (2)$$

where q_e and q_t are the sorption capacities at equilibrium and at time t, respectively (mg g^{-1}) and k_1 (min^{-1}) is the rate constant. The equation applicable to experimental results generally differs from a true first order equation in two ways [24]: (i) the parameter log (q_e-q_t) does not represent the number of available sites and (ii) the parameter log (q_e) is an adjustable parameter and often it is found not equal to the intercept of a plot of log (q_e-q_t) against t, whereas in a true first order log (q_e) should be equal to the intercept of a plot of log (q_e-q_t) against t. In order to fit Eq. (2) to experimental data, the equilibrium capacity, q_e, must be known. In many cases q_e is unknown and as chemisorption tends to become immeasurably slow, the amount sorbed is still significantly smaller than the equilibrium amount [25]. In over 50% of literature references, based on analyzing sorption kinetics, authors did not measure an equilibrium isotherm [26].

The data for the sorption of RhB onto BPH activated carbon were plotted according to Eq. (2) and the results are summarized in Table 5. The equilibrium capacity q_e was obtained by trial and error and the correlation coefficients are shown in Table 5 for the effect of pH, particle size, concentration and temperature. Numerous applications of the Lagergren equation (pseudo-first order systems) have been reported. Boyd et al. [27] proposed that: (i) if the film diffusion is rate controlling, the slope of the plots of Eq. (9) will vary inversely with the particle size, the film thickness and with the distribution coefficient, k; (ii) if the sorption rate-controlling step is chemical exchange, the slope will be independent of particle diameter and flow rate and will depend only on the concentration of the sorbate in solution and the temperature. In the case of the sorption of RhB onto BPH activated carbon, the rate constant is independent of concentration but dependent on temperature.

Table 6
Kinetic of adsorption of RhB onto BPH activated carbon: pseudo-second-order parameters for the effect of pH, particle sizes, concentration and temperature.

Parameter	Values	Second-order equation $t/q_t = 1/kq_e^2 + 1/q_e t$				
		q_e exp. mg g^{-1}	q_e calcu. mg g^{-1}	kg mg^{-1} min^{-1}	r^2	$h = kq_e^2$
pH	2.45	192.5	224.2	8.6×10^{-5}	0.994	4.323
	3.44	188.7	223.2	8.6×10^{-5}	0.992	4.284
	6.03	183.9	219.3	8.4×10^{-5}	0.992	4.039
	8.47	176.8	208.3	8.3×10^{-5}	0.993	3.601
	10.33	169.9	199.6	8.2×10^{-5}	0.993	3.266
Particle size (mm)	<0.25	200.0	239.2	7.4×10^{-5}	0.994	4.234
	<0.50	192.5	230.9	7.3×10^{-5}	0.994	3.892
	<1.00	188.7	229.9	6.8×10^{-5}	0.993	3.594
Concentration (mg l^{-1})	100	100.0	104.8	5.9×10^{-4}	0.998	6.479
	200	198.6	242.7	5.7×10^{-5}	0.992	3.357
	300	213.8	264.6	5.0×10^{-5}	0.997	3.501
	400	235.0	295.9	4.8×10^{-5}	0.995	4.203
	500	258.0	312.5	4.6×10^{-5}	0.997	4.492
	600	264.0	319.6	4.4×10^{-5}	0.996	4.494
Temperature (°C)	20	192.6	234.2	6.7×10^{-5}	0.994	3.675
	35	195.9	235.3	6.9×10^{-5}	0.994	3.820
	50	199.6	236.6	7.9×10^{-5}	0.994	4.311
	70	218.8	258.4	6.5×10^{-5}	0.995	4.340

The mechanism of RhB sorption onto BPH may be chemically rate controlling.

3.5.2. Pseudo-second-order reaction

If the rate of sorption is a second-order mechanism, the pseudo-second-order chemisorption kinetic rate equation is expressed as:

$$\frac{t}{q_t} = \frac{1}{kq_e^2} + \frac{1}{q_e}t \quad (3)$$

where q_e and q_t are the sorption capacities at equilibrium and at time t, respectively ($mg\,g^{-1}$) and k is the rate constant of pseudo-second-order sorption ($g\,mg^{-1}\,min^{-1}$). where h can be regarded as the initial sorption rate as $q_t/t \to 0$, hence:

$$h = kq_e^2 \quad (4)$$

Eq. (3) can be written as:

$$\frac{t}{q_t} = \frac{1}{h} + \frac{1}{q_e}t \quad (5)$$

Eq. (3) does not have the disadvantage of the problem with assigning an effective q_e. If pseudo-second-order kinetics are applicable, the plot of t/q_t against t of Eq. (3) should give a linear relationship, from which q_e, k and h can be determined from the slope and intercept of the plot and there is no need to know any parameter beforehand.

The application of second-order equation to the experimental results of adsorption of RhB onto BPH activated carbon, gives the highest values of the correlation coefficient of the three kinetic models under investigation: (i) *Effect of initial pH:* The highest value of correlation coefficient and initial sorption rate are obtained at the value of 2.45 of initial pH and decreased as the pH of solution increased confirming the experimental results obtained, where sorption capacity decreased from 224.2 to 199.6 $mg\,g^{-1}$ when the pH of the dye solution was increased from 2.45 to 10.33. (ii) *Effect of particle size of the adsorbent:* Table 6 illustrated that increasing the particle size of adsorbent from <0.25 to <1.00 mm leading to the decrease in adsorption capacity, adsorption rate, correlation coefficient and initial rate of adsorption. (iii) *Effect of initial dye concentration:* Table 6 shows the constants of Eq. (2) that were obtained from slope and intercept. All the fits show very good correlation coefficients. HO and McKay presented similar results for the sorption systems of basic and acid dyes onto pith [28]. The equilibrium sorption capacity q_e increased from 104.8 to 319.6 $mg\,g^{-1}$ when the initial concentration of RhB increased from 100 to 600 $mg\,l^{-1}$. But, the values of the rate constant were found to decrease from $5.9 \times 10^{-4--}$ to 4.4×10^{-5} $g\,mg^{-1}\,min^{-1}$ for an increase in the initial concentration and this is may be due to strike hindrance of higher concentration of dye. *(iv) Effect of temperature*: Table 6 shows the sorption kinetics of RhB removal at 20, 35, 50 and 70 °C at the initial dye concentration of 250 $mg\,l^{-1}$. Increasing the temperature from 20 to 70 °C, the removal of the dye increased from 234.2 to 258.4 $mg\,g^{-1}$. This may be due to a tendency for the dye molecules to escape from the bulk phase to the solid phase with an increase in temperature of the solution [29]. The temperature dependence of dye sorption by BPH activated carbon shows a good compliance with the pseudo-second-order equation, which is reflected by high coefficients of correlation as shown in Table 6. Fig. 7 shows a linear relationship between the logarithm of rate constant and the reciprocal of temperature. The activation energy (E) for the sorption of RhB by BPH sorbent was calculated using the Arrhenius equation [30]:

$$k = k_0 \exp\left(\frac{-E}{RT}\right) \quad (6)$$

where k ($g\,mg^{-1}\,min^{-1}$) is pseudo-second-order constant of sorption, k_0 is the temperature independent factor ($g\,mg^{-1}\,min^{-1}$), R is the gas constant ($8.314\,J\,mol^{-1}\,K^{-1}$), and T is the solution temperature (K).From this equation, the rate constant of sorption, k_0 is 3.865×10^{-4} $g\,mg^{-1}\,min^{-1}$ and the activation energy of sorption E is 62.03 $kJ\,mol^{-1}$.These findings show that dye adsorption process by BPH activated carbon is chemisorptions and endothermic process.

Table 7
Kinetic of adsorption of RhB onto BPH activated carbon: Elovich equation parameters for the effect of pH, particle sizes, concentration and temperature.

Parameter	Values	Elovich Equation $q_t = \beta \ln(a\,\beta) + \beta \ln(t)$		
		β	α	r^2
pH	2.45	45.08	0.00653	0.982
	3.44	44.69	0.00592	0.980
	6.03	44.11	0.00588	0.979
	8.47	41.61	0.00564	0.981
	10.33	39.45	0.00558	0.982
Particle size (mm)	<0.25	48.48	0.00433	0.982
	<0.50	47.29	0.00427	0.977
	<1.00	48.22	0.00362	0.976
Concentration ($mg\,l^{-1}$)	100	9.58	0.00101	0.949
	200	50.95	0.00226	0.983
	300	55.37	0.00270	0.974
	400	62.69	0.00277	0.971
	500	61.21	0.00363	0.994
	600	62.11	0.00401	0.989
Temperature (°C)	20	48.94	0.00358	0.985
	35	48.29	0.00401	0.985
	50	46.69	0.00515	0.986
	70	51.58	0.00518	0.988

3.5.3. Elovich model

The Elovich equation is generally expressed as follows [31]:

$$q_t = \beta \ln(\alpha\beta) + \beta \ln(t) \quad (7)$$

Where q_t is the sorption capacity at time t ($mg\,g^{-1}$), α is the initial sorption rate ($mg\,g^{-1}\,min^{-1}$) and β is the desorption constant ($g\,mg^{-1}$) during any experiment. Thus, the constants can be obtained from the slope and the intercept of a straight line plot of q_t against $\ln(t)$.

Table 7 lists the kinetic constants obtained from the Elovich equation. It will be seen from the data that the value of α and β varied as function of the pH, particle size of the adsorbent, initial dye concentration and temperature. (a) *Effect of initial pH of solution:* The values of α and β decrease as the pH of the solution increases, this is in agreement with the experimental results obtained. (b) *Effect of particle size of adsorbent:* As the particle size decreases the initial adsorption rate, α, increases, this is because higher surface area with smaller particle leads to higher initial adsorption rate confirming the results obtained from the second-order reaction listed in Table 6. (c) *Effect of initial dye concentration:* On increasing the initial dye concentration, the value of α, initial adsorption rate, increases and the value of β, desorption constant, decreases with the concentration more than 400 $mg\,l^{-1}$. (d) *Effect of temperature:* As the temperature increases from 20 to 70 °C, the value of α increases from 35.8×10^{-4} to 51.8×10^{-4}.

3.5.4. Intra-particle diffusion

Sorption of sorbate on sorbent proceeds in several steps, involving transport of the solute molecules from the aqueous phase to the surface of the solid particulates (film diffusion) and diffusion of the solute molecules into the interior of the pores, which is usually a slow process. The intra-particle diffusion rate constant (k_{id}) is given by the Weber–Morris equation [32]:

$$q_t = k_{idt}^{0.5} + I \quad (8)$$

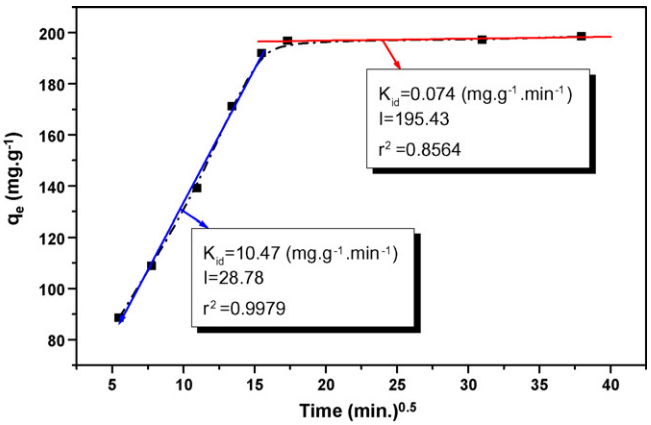

Fig. 8. Intra-particle diffusion of RhB through adsorption onto BPH activated carbon.

where k_{id} is the rate constant of intra-particle transport in mg g^{-1} min$^{1/2}$ and I, is the boundary layer (film diffusion). When intra-particle diffusion plays a significant role in controlling the kinetics of the sorption process, the plots of q_t versus $t^{0.5}$ yield a straight line passing through the origin and the slope gives the rate constant, k_{id}.

The sorption of RhB onto the BPH activated carbon depends on film diffusion and intra-particle diffusion, and the more rapid one will control the overall rate of transport. Thus, the concentration of the sorbed RhB, q_t (mg g^{-1}) was plotted against time applying the Weber–Morris equation as shown in Fig. 8. According to the intra-particle diffusion model, a linear plot indicates a rate controlled by intra-particle diffusion. This is due to the fact that fractional uptake will vary with the function k_{id} $(t)^{0.5}$. In contrast, the plot obtained from this study shows multi-linearity with 2 steps. The first part of the multi-linear plot is attributed to boundary layer diffusion, the second to the intra-particle diffusion and the chemical reaction. The multi-linearity curve indicates that intra-particle diffusion is not a fully operative mechanism in the sorption of RhB by the BPH.

The diffusion rate was found high in the initial stages (k_{id} = 10.47 mg g^{-1} min^{-1}) and decreased on passage of time (k_{id} = 0.074 mg g^{-1} min^{-1}), indicating that the rate of the adsorption step is film diffusion at the early stage of removal of dye. The value of k_{id} indicated that intra-particle diffusion step could be a rate-controlling step. The change in the slope may be due to the existence of different pore sizes [33]. This behavior was also confirmed from the linear plot of B_t versus time employing Reichenburg equation [34]:

$$B_t = -0.4977 - 2.303 \log(1 - F) \quad (9)$$

Where B_t is a mathematical function (F) of q_t/q_e. The plot was linear up to 120 min and does not pass through the origin (correlation coefficient, $r^2 = 1$).

3.6. Sorption isotherm studies

Adsorption isotherms are important for the description of how adsorbates will interact with an adsorbent and are critical in optimizing the use of adsorbent. Thus, analysis of the results obtained from the equilibrium isotherm studies is fundamental to evaluate the affinity of the adsorbent for a particular adsorbate. Equilibrium studies are described by a sorption isotherm characterized by certain constants whose values express the surface properties and affinity of the adsorbent. Consequent upon this, the results obtained from these studies were tested with 5 different isotherm equations (i.e. Langmuir, Freundlich, Temkin, Halsey, and Harkins–Jura isotherm equations): (1) The monolayer coverage of the adsorbate on the adsorbent surface at constant temperature is represented by the Langmuir isotherm. The Langmuir isotherm hints towards surface homogeneity. The linearized form of the equation can be represented thus [35];

$$\frac{C_e}{q_e} = \frac{1}{kq_m} + \left[\frac{x}{q_m}\right] C_e \quad (10)$$

where C_e is the concentration of the adsorbate at equilibrium (mg l^{-1}), q_e is the amount of adsorbate adsorbed at equilibrium per unit mass of adsorbent (mg g^{-1}), q_m is the monolayer sorption capacity at equilibrium (mg g^{-1}), and k is the Langmuir equilibrium constant (l mg^{-1}). A plot of C_e/q_e versus C_e gives a straight line, if the sorption process is described by the Langmuir isotherm equation. The values of q_m and k are obtained from the slope and intercept of the straight line plot. (2) The Freundlich isotherm is regarded as an empirical isotherm. It indicates the surface heterogeneity of the adsorbent. The linearized form of the isotherm is expressed thus;

$$\ln q_e = \ln K_f + \frac{1}{n \ln C_e} \quad (11)$$

Where k_f and n are Freundlich coefficients, obtainable from the plots of $\ln q_e$ versus $\ln C_e$. k_f and n are Freundlich adsorption constants, related to adsorption capacity and sorption intensity, respectively. (3) Temkin and Pyzhev [36] studied the heat of adsorption and the adsorbent–adsorbate interaction on surfaces [36]. The Temkin isotherm equation is given as:

$$q_e = B_1 \ln K_T + B_1 \ln C_e \quad (12)$$

where $B_1 = RT/b$, T (K) is the absolute temperature, R is the universal gas constant (8.314 J mol^{-1}), K_T is the equilibrium binding constant (l mg^{-1}), and B_1 is related to the heat of adsorption. The Temkin constants are obtained from the plot of q_e versus $\ln C_e$. (4) The Harkin–Jura[37] adsorption isotherm can be expressed as:

$$\frac{1}{q_e^2} = \left(\frac{B}{A}\right) - \left(\frac{1}{A}\right) \log C_e \quad (13)$$

the isotherm equation accounts for multilayer adsorption and can be explained by the existence of a heterogeneous pore distribution. (5) The Halsey adsorption isotherm (Halsey) [38] can be given as:

$$\ln q_e = \left(\frac{1}{n} \ln k\right) - \frac{1}{n} \ln C_e \quad (14)$$

this equation is suitable for multilayer adsorption and the fitting of the experimental data to this equation attest to the heteroporous nature of the adsorbent.

Results of adsorption isotherms showed the shape of type L (Fig. 9) according to the classification of Giles et al. [30]. The L (or Langmuir) shape of the isotherms means that there is no strong

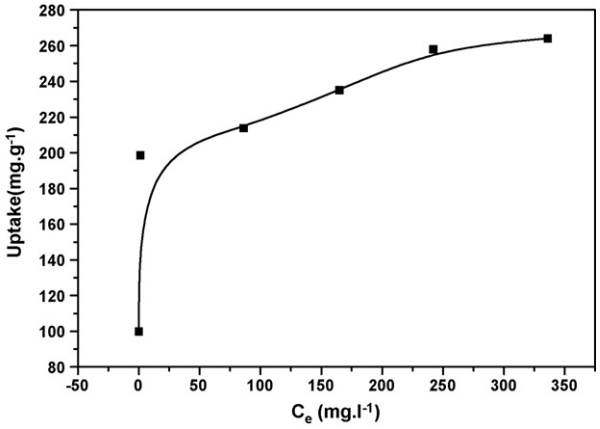

Fig. 9. Adsorption isotherm of RhB dye onto BPH activated carbon.

Table 8
Langmuir parameters at different conditions.

Langmuir parameters at different temperatures and constants concentration (200 mg l^{-1}).					Langmuir parameters at different concentrations and constant temperatures		
	20 °C	35 °C	50 °C	70 °C	At 20 °C	R_L [$R_L = 1/1 + bC_0$]	C_0 (mg l^{-1})
q_m (mg g^{-1})	93.1	98.23	103.6	119.3	263.85	0.072	100
b (l mg^{-1})	0.142	0.1862	0.258	0.0616	0.1286	0.025	300
r^2	0.982	0.983	0.979	0.991	0.9970	0.013	600

Table 9
Parameters of different isotherms of adsorption of RhB onto BPH activated carbon.

Freundlich isotherm	Temkin isotherm	Harkins–Jura isotherm	Halsey isotherm
$K_f = 158.5$ (l g^{-1})	$B = 14.1$	$A = 0.5835$	$n = 11.33$
$n = 10$	$K_T = 172.7$ (l mg^{-1})	$B = 3.095$	$K = 154.58$
$r^2 = 0.9595$	$r^2 = 0.9656$	$r^2 = 0.922$	$r^2 = 0.989$

competition between the solvent and the adsorbate to occupy the adsorbent sites. In this case, the longitudinal axes of the adsorbed molecules are parallel to the adsorbent surface [30]. The results obtained were analyzed using 5 different isotherm equations. In order to understand the mechanism of RhB adsorption onto BPH, the experimental data were fitted to the aforementioned equilibrium isotherm equations and the different isotherm parameters, obtained from the different plots, are presented in Tables 8 and 9. An error function is required to evaluate the fitness of each isotherm equation to the experimental data obtained from the optimization process employed. In the present study the linear coefficient of determinations, r^2, was used. The values of the linear correlation, r^2, of each isotherm equation, when fitted to the experimental data are presented in Tables 8 and 9. The highest values of r^2 were obtained when the experimental data were fitted into Langmuir and Halsey isotherm equations. The description of the sorption of RhB onto BPH by the Langmuir isotherm equations is a pointer to: (i) the monolayer coverage of the sorbate on a sorbent surface at constant temperature, (ii) homogeneity of the surface of the BPH. and (iii) q_m and b were determined from the slope and intercept of the plot (Figs. 10 and 11) and are presented in Table 8. Their values were found to be 263.85 $^-$and 0.1286 (l mg^{-1}), respectively. R_L values between 0.0 and 1.0 at different concentrations indicate favorable adsorption of dye onto BPH activated carbon (Table 10). Halsey isotherm hints towards the aggregation (or agglomeration) of the zwitterionic form of RhB in water to form a larger molecular form (dimer) (Fig. 5) at the surface of the BPH activated carbon.

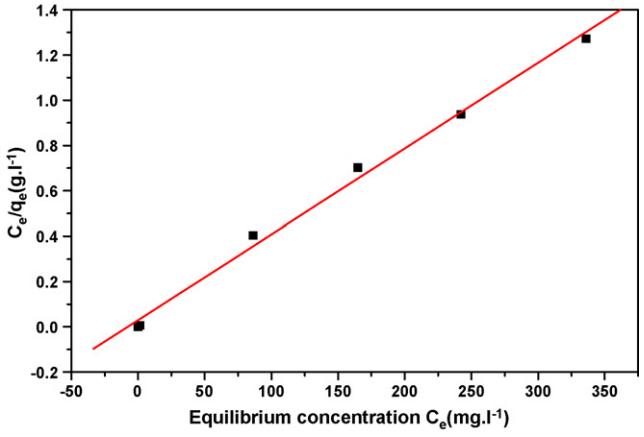

Fig. 10. Linear from of Langmuir equation of adsorption of RhB onto BPH adsorbent at different concentrations and constant temperatures.

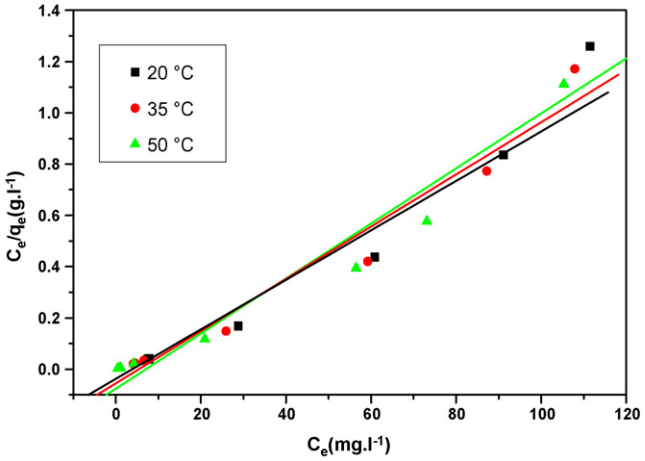

Fig. 11. Linear from of Langmuir equation of adsorption of RhB onto BPH adsorbent at different temperatures and constant concentrations.

3.7. Effect of particle size

It is clear that with the decrease in particle size, the sorption increases because the sorption capacity is directly proportional to the total exposed surface and inversely proportional to particle diameter for a non-porous sorbent [15]. This is due to the fact that sorption being a surface phenomenon; the smaller sorbent sizes offered comparatively larger surface area and hence higher RhB removal at equilibrium as shown in Fig. 12. This can be explained by the fact that for smaller particles, large external surface area is presented to the RhB molecules in the solution which results in a lower driving force per unit surface area for mass transfer than when larger particles used [39].

3.8. Effect of temperature

The plot of adsorption capacity as a function of temperature (Fig. 13) shows an increasing amount of adsorbed RhB with temperature from 20 to 70 °C indicating that adsorption capacity depends

Table 10
Constant parameter, R_L.

R_L Value	Type of isotherm
$R_L > 1.0$	Unfavorable
$R_L = 1.0$	Linear
$R_L = 0.0$	Irreversible
$0.0 < R_L < 1.0$	Favorable

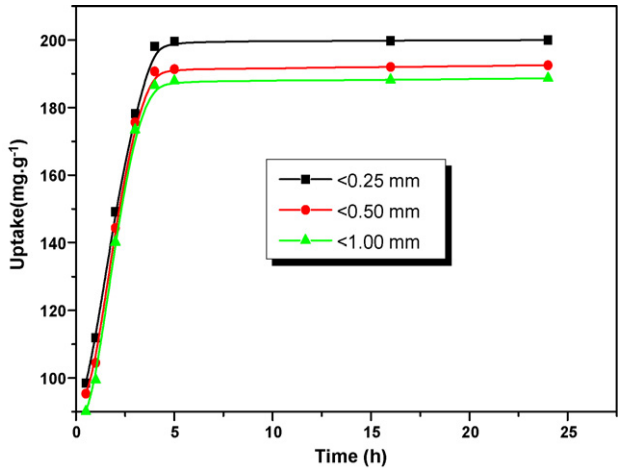

Fig. 12. Effect of particle size on the adsorption of RhB onto BPH activated carbon.

on temperature. The molecular size of RhB [13] (L: 1.8 nm; B: 0.7 nm) and the average pore size of the carbon are near to 2 nm. Therefore, after the pore has adsorbed RhB molecules at the opening, it will hinder the subsequent entrance of RhB molecules. The intra-particle diffusion rate of sorbate into the pores will be intensified as temperature increases, as diffusion is an endothermic process [40]. So the adsorption increases with temperature.

3.8.1. Thermodynamic studies

The uptake of RhB dye by the BPH increases on raising the temperature confirming the endothermic nature of the adsorption step. The change in standard free energy (ΔG^0), enthalpy (ΔH^0) and entropy (ΔS^0) of adsorption were calculated from the following equations:

$$\Delta G = -RT \ln K_C \quad (15)$$

where R is the gas constant, K_C the equilibrium constant and T the temperature in K. The K_C value is calculated from Eq.;

$$K_C = \frac{C_A}{C_S} \quad (16)$$

Where C_A and C_S are the equilibrium concentrations of dye ions on adsorbent ($mg\,l^{-1}$) and in the solution ($mg\,l^{-1}$), respectively. Standard enthalpy (ΔH) and entropy (ΔS), of adsorption can be estimated from van't Hoff equation given in:

$$\ln K_C = \frac{-\Delta H}{RT} + \frac{\Delta S}{R} \quad (17)$$

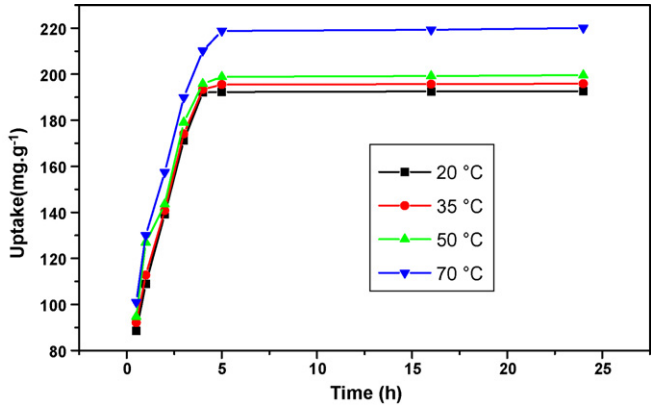

Fig. 13. Effect of temperature on the adsorption of RhB onto BPH activated carbon.

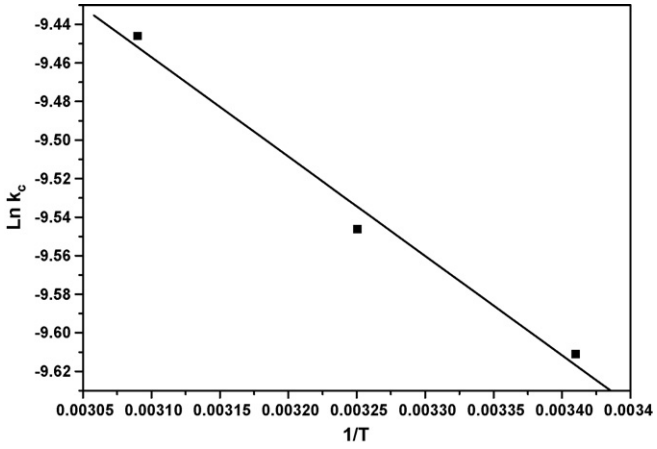

Fig. 14. Plot of $\ln k_c$ against reciprocal temperature for RhB sorption onto BPH activated carbon.

Table 11
The thermodynamic parameters of the adsorption of RhB using BPH activated carbon.

Temperature (K)	$-\Delta G$ ($kJ\,mol^{-1}$)	ΔH ($kJ\,mol^{-1}$)	ΔS($J\,mol^{-1}\,K^{-1}$)
293	7.939	4.151	65.786
308	9.902		
323	12.361		
343	26.729		

The slope and intercept of the van't Hoff plot is equal to $-\Delta H/R$ and $\Delta S/R$, respectively [30]. The van't Hoff plot for the adsorption of RhB onto BPH is given in Fig. 14. Thermodynamic parameters obtained are summarized in Table 11. From Table 11, the positive values of enthalpy change ($\Delta H = 4.151\,kJ\,mol^{-1}$) conform the endothermic nature of the adsorption process. The positive value of ΔS ($\Delta S = 65.786\,J\,mol^{-1}\,K^{-1}$) reflects the affinity of adsorbent material towards RhB. Despite being endothermic nature, the spontaneity of the adsorption process was decreased in the Gibbs energy of the system. The ΔG values varied in range with the mean values showing a gradual increase from −7.939 to −26.729 ($kJ\,mol^{-1}$) in the temperature range of 20–70 °C in accordance with the endothermic nature of the adsorption process.

3.9. Desorption studies of RhB dye

Desorption studies help to elucidate one mechanism of adsorption and recovery of the adsorbate and adsorbent. The regeneration of the adsorbent may make the treatment process economical. If the adsorbed dyes can be desorbed using neutral pH water, then the attachment of the dye to the adsorbent is by weak bonds. If acid or alkaline water desorps the dye then the adsorption is by ion exchange. If organic acids, like acetic acid can desorp the dye, then the dye is held by the adsorbent through chemisorption [41]. The effect of various reagents used for desorption studies indicates that NaOH is a better reagent for desorption, because we could get 7.8, 5.4 and 2.7% removal of adsorbed dye for NaOH, HCl and H_2O, respectively after 24 h of contact between the loaded matrix and the desorbing agents. This is expected because desorption will depend on the size of the molecule, number of contact points, surface concentration, temperature and concentration of adsorbed species in solution [42]. In absence of competition from other adsorbates, large adsorbed molecules are unlikely to desorp on dilution with water [43]. Such molecules will have several contact points leading to large net adsorption energy, although individual contacts may be weak. It is therefore statistically and energetically improbable that all segments will leave the surface simultaneously [42]. In

Table 12
The estimated costs of prepared BPH and commercial activated carbon.

No.	Item	Costs (pt.)	US $
1	Raw material (transportation and crushing included).	50	0.09
2	Commercial H_3PO_4 (L) = (1.167 L for 1 kg)	240 × 1.167 = 280	0.507
3	Power consumption (4 h × 1.8 kW × 20 pt.)	144	0.261
4	Water	30	0.05
5	Personnel	40	0.07
6	Total for 1 kg of prepared activated carbon	544	$0.978 ≈ 1.00
7	Total for 1 ton prepared activated carbon	$1000	
8	Total for 1 kg of commercial activated carbon	2500	$4.55
9	Total for 1 ton of commercial activated carbon	$4550	

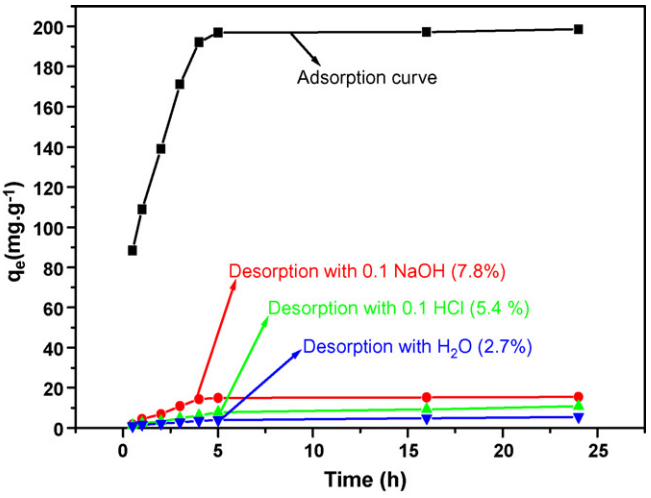

Fig. 15. Adsorption and desorption curves of RhB by BPH activated carbon.

particular, adsorption on a porous substance such as activated carbon may take place in pores of a diameter similar to that of the adsorbing species. consequently, there could be many contact points and a correspondingly high adsorption energy. For desorption to take place, a large energy barrier may need to be overcome [43]. In conclusion, it may be noted that the kinetic tests suggested the reversibility of the adsorption process is incomplete (Fig. 15). So, the regeneration of activated carbon can be made by thermal treatment at elevated temperatures.

3.10. Cost analysis

The relative cost of the material used in the present study is very much lower than that of commercial activated carbons as shown in Table 12. The bagasse pith is available abundantly; throughout the year, free of cost, and after considering expenses like transport, chemical, electrical energy and processing cost, the cost of the material would be approximately US $ 1/kg (US $1000/ton)[46]. This cost can be further brought down after successful regeneration of used activated carbon. The cost of the activated carbon used for water treatment in our country is more than US $4.55/kg (US $4550/ton).

4. Conclusion

This study shows the application of activated carbon prepared from bagasse pith for removal of Rhodamine B from aqueous solution. From the experimental results it was found that: (1) the bagasse pith treated with phosphoric acid (BPH) showed higher adsorption capacity for adsorption of Rhodamine B (RhB) than the treated with potassium hydroxide (BPK). The maximum removal of dye was observed at pH 2.45. The adsorption capacity increases with the decrease in particle size due to the increase in the surface area. The equilibrium time was 240 min. The effect of temperature revealed that the adsorption of the dye, RhB is an endothermic indicating that the adsorption would be enhanced at temperature above the ambient temperature. (2) According to Langmuir adsorption isotherm, the adsorption capacity, q_m, is 263.85 (mg g^{-1}) at initial pH 5.7 for the particle size of 0.25 nm and equilibrium time of 240 min at a temperature of 20 °C and initial dye concentration range of 100–600 (mg l^{-1}). (3) The adsorption of RhB from aqueous solution onto BPH proceeds according to the pseudo-second-order and the dye uptake process was found to be controlled by film diffusion at earlier stages and by intra-particle diffusion at later stages. (4) Desorption studies carried out in water medium, HCl and NaOH with desorption of 2.7, 5.4 and 7.8% respectively of adsorbed RhB confirming the chemical adsorption mechanism of the dye. This adsorbent was found to be both effective and economically viable.

References

[1] R. Malik, D.S. Ramteke, S.R. Wate, Adsorption of malachite green on groundnut shell waste based powdered activated carbon, Waste Manag. 27 (9) (2007) 1129–1138.
[2] V.K. Garg, M. Amita, R. Kumar, R. Gupta, Basic dye (methylene blue) removal from simulated wastewater by adsorption using Indian rosewood saw dust: a timber industry waste, Dyes Pig. 63 (2004) 243–250.
[3] T. Robinson, G. McMullan, R. Marchant, P. Nigam, Remediation of dyes in textile effluent: a critical review on current treatment technologies with a proposed alternative, Bioresour. Technol. 77 (2001) 247–255.
[4] R.R. Bansode, J.N. Losso, W.E. Marshall, R.M. Rao, R.J. Portier, Adsorption of metal ions by pecan shell based granular activated carbons, Bioresour. Technol. 89 (2003) 115–119.
[5] K. Ankur, G. Collin, J. Faujan, B.H. Ahmad, Z. Zulkarnian, Z.M. Hussain, H.A. Abdullah, Preparation and characterization of activated carbon from Resak wood (Vatika hulletti), Res. J. Chem. Environ. 5 (3) (2001) 21–24.
[6] W.T. Tsai, C.Y. Chang, S.Y. Wang, C.F. Chang, S.F. Chien, H.F. Sun, Cleaner production of carbon adsorbents by utilizing agricultural waste corn cob Resources, Conservation Recycling 32 (2000) 43–53.
[7] A. Ahmadpour, D.D. Do, The preparation of active carbons from coal by chemical and physical activation, Carbon 34 (4) (1996) 471–479.
[8] M.A. Lillo-Rodensas, D. Carzrola-Ameros, A. Linares-Solano, Chemical reactions between carbons and NaOH and KOH––an insight into chemical activation mechanisms, Carbon 41 (2003) (2003) 265–267.
[9] G. Mckay, Application of surface diffusion model to the adsorption of dyes on bagasse pith, Adsorption 4 (1998) (1998) 361–372.
[10] S.M. Saad, A.M. Nasser, M.T. Zimaity, H.F. Abdel-Maged, J. Oil Colour Chem. Ass. 61 (1978) 43.
[11] H. Lata, V.K. Garg, R.K. Gupta, Removal of a basic dye from aqueous solution by adsorption using parthenium hysterophorus: an agricultural waste, Dyes Pig. 74 (2007) 653–658.
[12] C. Moreno-Castilla, M.A. Ferro-Garcia, Activated carbon surface modifications by nitric acid, hydrogen peroxide, and ammonium peroxydisulfate treatments, Langmuir 11 (11) (1995) 4386–4392.
[13] Y. Guo, J. Zhao, H. Zhang, S. Yang, J. Qi, Z. Wang, H. Xu, Use of rice husk-based porous carbon for adsorption of Rhodamine B from aqueous solutions, Dyes Pig. 66 (2005) 123–128.
[14] B. Puri, O. Mahajan, Soil Sci. 94 (1962) 162.
[15] S.N. Preeti, B.K. Singh, N. Siddarth, Equilibrium, Kinetic and thermodynamic studies on phenol sorption to clay, J. Environ. Prot. Sci. 1 (2007) 83–91.
[16] A.V. Deshpande, U. Kumar, Effect of method of preparation on photophysical properties of Rh-B impregnated sol–gel hosts, J. Non-Cryst. Solids 306 (2) (2002) 149–159.
[17] A. Ghanadzadeh, M.A. Zanjanchi, R. Tirbandpay, The role of host environment on the aggregative properties of some ionic dye materials, J. Mol. Struct. 616 (1e3) (2002) 167–174.

[18] I. Lopez Arbeloa, P. Ruiz, Ojeda, Dimeric states of Rhodamine B, Chem. Phys. Lett. 87 (6) (1982) 556–560.
[19] C. Lin, A.R. James, N.P. Branko, Correlation of double-layer capacitance with the pore structure of sol–gel derived carbon xerogels, J. Electrochem. Soc. 146 (10) (1999) 3639–3643.
[20] K.S. Low, C.K. Lee, L.L. Heng, Sorption of basic dyes by Hydrilla verticillata, Environ. Technol. 14 (1993) 115–124.
[21] V.K. Garg, A. Moirangthem, R. Kumar, R. Gupta, Basic dye (methylene blue) removal from simulated wastewater by adsorption using Indian rosewood sawdust: timber industry waste, Dyes Pig. 63 (2004) 243–250.
[22] C. Namasivayam, J.S.E. Arasi, Removal of Congo red from wastewater by adsorption onto waste red mud, Chemosphere 34 (1997) 401–417.
[23] S. Lagergren, About the theory of so-called adsorption of soluble substances, Kungliga Svenska Vetenskapsakademiens. Handlingar 24 (4) (1898) 1–39.
[24] C. Aharoni, D.L. Sparks, Kinetics of soil chemical reactions-a theoretical treatment, in: D.L. Sparks, D.L. Suarez (Eds.), Rates of Soil Chemical Processes, Soil Science Society of America, Madison, WI, 1991, pp. 1–18.
[25] M. Ungarish, C. Aharoni, Kinetics of chemisorption: deducing kinetic laws from experimental data, J. Chem. Soc.-Faraday Trans. 77 (1981) 975–985.
[26] Y.S. Ho, G. Mckay, A comparison of chemisorption kinetic models applied to pollutant removal on various sorbents, Trans. IChemE 76 (B) (1998).
[27] G.E. Boyd, A.W. Adamson Jr., L.S. Myers, The exchange adsorption of ions from aqueous solutions by organic zeolites. II. Kinetics, J. Am. Chem. Soc. 69 (1947) (1947) 2836–2848.
[28] G. Mckay, M.S. El guendi, M.M. Nassar, Equilibrium studies for the adsorption of dyes on bagasse pith, J. Adsorption Sci. Technol. 15 (1997) 251–270.
[29] Y.S. Ho, C.C. Chiang, Sorption studies of acid dye by mixed sorbent, Adsorption J. Int. Adsorption Soc. 7 (2001) 139–147.
[30] C.H. Giles, T.H. MacEwan, S.N. Nakhwa, D. Smith, Studies in adsorption. Part XI. A system of classification of solution adsorption isotherms, and its use in diagnosis of adsorption mechanisms and in measurements of specific surface areas of solids, J. Chem. Soc. 10 (1960) 3973–3993.
[31] M.J.D. Low, Kinetics of chemisorption of gases on solids, Chem. Rev. 60 (1960) 267–312.
[32] W.J. Weber, J.C. Morris, J. Sanit. Eng. Div. Am. Soc. Civ. Eng. 90 (SA3) (1964) 70.
[33] S.L.C. Ferreira, H.C. Dos Santos, M.S. Fernandes, J. Anal. Atom. Spectrom. 17 (2002) 115.
[34] D. Reichenburg, J. Am. Chem. Soc. 75 (1972) 589.
[35] N.A. Oladoja, I.O. Asia, C.O. Aboluwoye, Y.B. Oladimeji, A.O. Ashogbon, Studies on the sorption of basic dye by rubber (hevea brasiliensis) seed shell, Turk. J. Eng. Env. Sci. 32 (2008) 1–10.
[36] M.I. Temkin, V. Pyzhev, Kinetic of ammonia synthesis on promoted iron catalysts, Acta Physiochim. URSS 12 (1940) 327–356.
[37] W.D. Harkirns, G.J. Jura, The decrease of free surface energy as a basis for the development of equations for adsorption isotherms; and the existence of two condensed phases in films on solids, J. Chem. Phys. 12 (1944) 112–113.
[38] J. Halsey, Chem. Phys. 16 (1948) 931.
[39] M. Ozacar, I.A. Sengil, Adsorption of acid dyes from aqueous solutions by calcined alunite and granular activated carbon, Adsorption 8 (2002) 301–308.
[40] G.N. Manju, M.C. Giri, Indian J. Chem. Technol. 6 (1) (1999) 134–140.
[41] S. Arivoli, M. Thenkuzhali, Kinetic, mechanistic, thermodynamic and equilibrium studies on the adsorption of Rhodamine B by acid activated low cost carbon, E-J. Chem. 5 (2) (2008) 187–200.
[42] Th. Tadros, Polymers in Colloid Systems: Adsorption, Stability and Flow, Elsevier, Amsterdam, 1998.
[43] A.A.M. Daifullah, B.S. Girgis, H.M.H. Gad, A study of the factors affecting the removal of humic acid by activated carbon prepared from biomass material, Colloids Surf. A: Physicochem. Eng. Aspects 235 (2004) 1–10.
[44] N.K. Amin, Removal of reactive dye from aqueous solutions by adsorption onto activated carbons prepared from sugarcane bagasse pith, Desalination 223 (2008) 152–161.
[45] G. Mckay, M. El Geundi, M.M. Nassar, Pore Diffusion during the adsorption of dyes onto bagasse pith, Process Safety Environ. Prot. 74 (4) (1996) 277–288.
[46] http://www.financialexpress.com/news/phosphoric-acid-report-an-acid-test-for-manufacturers/159377/.